Proceedings of the 16th Czech and Slovak Conference on Magnetism, Košice, Slovakia, June 13–17, 2016

Structural Relaxation in the Amorphous Alloys: FeMeMoCrNbB (where Me = Ni or Co)

J. Rząckі[a], K. Błoch[a,*] and S. Walters[b]

[a]Faculty of Production Engineering and Materials Technology, Częstochowa University of Technology, 19 Armii Krajowej Av., 42-200 Częstochowa, Poland

[b]School of Computing, Engineering and Mathematics, University of Brighton, Cockcroft Building, Lewes Road, Brighton BN2 4GJ

In this paper, the results of structural and magnetic investigations are presented for the following amorphous alloys: FeMeMoCrNbB (where Me = Ni or Co). The structural investigations were performed using X-ray diffractometry. It was found that the investigated samples were amorphous in the as-cast state. The magnetisation was measured within magnetic fields ranging from 0 to 1 T using a vibrating sample magnetometer. Investigation of the "magnetisation in the area close to ferromagnetic saturation" showed that the magnetisation process in strong magnetic fields is connected with the rotation of magnetic moments in the vicinity of defects, which are the sources of short-range stresses. Analysis of the high-field magnetization curves facilitated the calculation of the spin-wave stiffness parameter.

DOI: 10.12693/APhysPolA.131.720

PACS/topics: 75.50.–y, 75.50.Kj, 75.30.Ds, 75.20.En, 75.47.Np, 75.50.Bb, 75.60.Ej

1. Introduction

Amorphous alloys are characterised by a lack of long-range atomic order. However, taking into account single atoms, short-range order could be found in the structure of amorphous materials. This order can be observed within distances comparable with the interatomic spacing. Spatial atomic order in these alloys is called "topological short-range order" (TSRO). If this order is extended to different types of atoms (in alloys composed of two- or more component elements), then it is called chemical short-range order (CSRO) [1]. The structural fluctuations present in amorphous alloys lead to the creation of structural defects [2–4]. Amorphous alloys consist inherently of atoms featuring different diameters; therefore, the type and volume of the resulting structural defects depend strongly on the chemical composition of each individual alloy. The structural fluctuations occurring in amorphous materials depend also on the selected manufacturing and thermal annealing conditions. Production methods involving the rapid quenching of the molten alloy at cooling rates of the order of 10^6 K/min result in the "freezing" of randomly distributed "free volumes" within the resulting amorphous structure. However, the configuration of these defects is not stable and, even during the solidification process, partial relaxation of these defects can occur; the associated mechanisms include: migration of defects, annihilation of defects, substitution with different defects, and conglomeration of point defects ("free volumes"). Three-dimensional conglomerations of point defects are unstable and are subject to a decomposition process, which creates linear defects — so-called "quasi-dislocational dipoles" [5, 6].

One method for investigation of the magnetisation of a material is the measurement of the magnetisation in strong magnetic fields. According to the Kronmüller theorem [7–9], the magnetisation ($\mu_0 M$) of an amorphous alloy in a strong magnetic field ($\mu_0 H$) can be described by the following equation, which is called the "law of approach to saturation":

$$\mu_0 M(H) = \mu_0 M_S \left(1 - \sum_{n=1}^{4} a_{n/2} \Big/ \mu_0 H^{n/2}\right) + \chi \mu_0 H + b(\mu_0 H)^{1/2}, \quad (1)$$

where M_s — saturation magnetization, μ_0 — magnetic permeability of a vacuum, H — magnetic field, $a_{1/2}, a_1, a_2$ — gradient coefficients of the linear fit related to the type of defect, b — gradient coefficient of the linear fit related to thermal dumping of the spin-waves by the strong magnetic field.

The factor b is related to the spin-wave stiffness parameter D_{spf} by the following relationship [10]:

$$b = 3.54 g \mu_0 \mu_B \left(\frac{1}{4\pi D_{spf}}\right)^{3/2} kT (g\mu_B)^{1/2}, \quad (2)$$

where g — the Lande split coefficient, μ_B — the Bohr magneton.

Parameter D_{spf} is described by the following equation [11]:

$$D_{spf} = 1/3 S J_{ex}(a) a^2 z_m, \quad (3)$$

where S — the spin value at the distance from the central atom, J_{ex} — the local exchange integral, a — the distance to the nearest-neighbour atoms, z_m — the quantity of magnetic atoms in the nearest neighbourhood.

The aim of this work was to determine the type of structural defects, influencing the magnetisation proces-

*corresponding author; e-mail: 23kasia1@wp.pl

ses of the amorphous alloys: $Fe_{60}Co_{10}Mo_5Cr_4Nb_6B_{15}$ and $Fe_{60}Ni_{10}Mo_5Cr_4Nb_6B_{15}$, in addition to ascertaining the respective spin-wave stiffness parameters (D_{spf}) thereof.

2. Materials and methods

The investigated alloy samples were produced in the form of ribbons with approximate dimensions: width 1 cm and thickness 20 μm. To achieve this, ingots of the required alloys, with the nominal compositions of $Fe_{60}Co_{10}Mo_5Cr_4Nb_6B_{15}$ and $Fe_{60}Ni_{10}Mo_5Cr_4Nb_6B_{15}$, were cast by melting high-purity component elements (Fe — 99.98%, Co — 99.99%, Mo — 99.9999%, Cr — 99.99%, Nb — 99.9999%, Ni — 99.99%) in an induction furnace. The element boron was added in the form of an alloy of known composition: $Fe_{45.4}B_{54.6}$.

Then, the amorphous ribbons were created using the "melt-spinning" technique, which involves the injection of the molten material onto a rotating cylinder. The casting and melt-spinning processes were performed under a protective argon atmosphere.

The structure of the obtained alloys was investigated by means of a Bruker D8 Advance X-ray diffractometer with a copper anode. The measurement of the isothermal magnetisation curves was achieved using a vibrating sample magnetometer.

The obtained alloys are paramagnetic at room temperature. Therefore, in order to determine the presence and type of defects, and to evaluate their effect on the magnetisation process, isothermal magnetisation curves were recorded for the following conditions: a temperature value of 250 K, and a maximal value of induction of the magnetising field of 1 T.

3. Results and discussion

Figure 1 shows the X-ray diffraction patterns obtained for the samples of the investigated alloys.

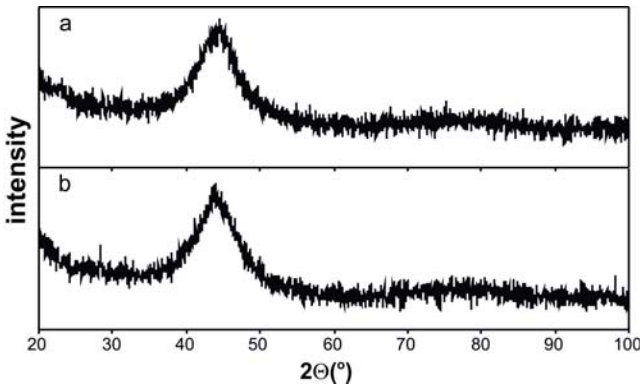

Fig. 1. The X-ray diffraction patterns for: (a) $Fe_{60}Co_{10}Mo_5Cr_4Nb_6B_{15}$ and (b) $Fe_{60}Ni_{10}Mo_5Cr_4Nb_6B_{15}$.

On examination of the obtained diffraction patterns, a wide maximum is visible at the 2Θ angle $\approx 44°$; this is typical for amorphous alloys.

The magnetisation curves for the investigated alloys are presented in Fig. 2.

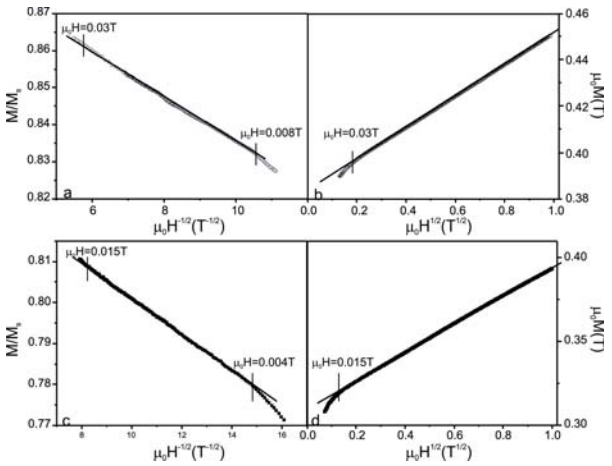

Fig. 2. High-field magnetisation curves, as a function of magnetic field induction, for the investigated amorphous alloys: $Fe_{60}Co_{10}Mo_5Cr_4Nb_6B_{15}$ (a, b) and $Fe_{60}Ni_{10}Mo_5Cr_4Nb_6B_{15}$ (c, d).

In the case of the alloy with added Co, over the magnetic field range of 0.008 T to 0.03 T, the following linear relationship is present (Fig. 2a): $M/M_S(\mu_0 H)^{-1/2}$.

This confirms that, within this field range, the magnetisation process is related to microscopic rotations of magnetic moments in the vicinities of point defects [12]. In higher magnetic fields, i.e. > 0.03 T, a different linear relationship is observed (Fig. 2b): $M(\mu_0 H)^{1/2}$. This indicates the presence of the Holstein–Primakoff paraprocess, related with the dumping of thermally induced spin-waves [13].

Similar relationships were observed for the second of the investigated alloys. In lower magnetic fields, in the vicinity of ferromagnetic saturation, the linear relationship of reduced magnetisations of: $M/M_S(\mu_0 H)^{-1/2}$ was observed. This indicates that, within the magnetic field range of 0.004 T to 0.015 T, point defects constitute the predominant influence on the magnetisation process. In stronger magnetic fields (greater than 0.015 T), the Holstein–Primakoff paraprocess was observed.

Parameters calculated from analysis of the magnetisation curves are presented in Table I.

TABLE I

The parameters obtained from analysis of the magnetisation curves: $a_{1/2}$ — coefficient related to the presence of structural defects, b — factor related to the Holstein–Primakoff paraprocess, D_{spf} — the stiffness parameter of the spin wave.

Parameters	$a_{1/2}$	b	D_{spf}
Sample	$[T^{-1/2}]$		$[10^{-2}$ eV nm$^2]$
$Fe_{60}Co_{10}Mo_5Cr_4Nb_6B_{15}$	0.006	0.075	37
$Fe_{60}Ni_{10}Mo_5Cr_4Nb_6B_{15}$	0.004	0.085	34

Analysis of the initial magnetisation curves in the region of the Holstein–Primakoff paraprocess allowed

the determination of the spin-wave stiffness parameter D_{spf}. The larger value of this parameter for the alloy with added Co indicates a larger quantity of magnetic atoms and smaller distances between them. This means a higher packing density of magnetic atoms is present in this alloy [14, 15]. This could be connected with the creation of CSRO.

4. Conclusions

The microstructure and magnetic properties of ribbon samples of the amorphous alloys, $Fe_{60}Co_{10}Mo_5Cr_4Nb_6B_{15}$ and $Fe_{60}Ni_{10}Mo_5Cr_4Nb_6B_{15}$, have been investigated and presented. The amorphicity of the investigated materials was confirmed by X-ray studies.

The effect of the alloying component on the type of structural defects in the approach to saturation region has been studied. The curves of the initial magnetisation have been analysed, according to the Kronmüller theorem. It has been found that, for both of the investigated alloys, the predominant role in the magnetisation process when under the influence of strong magnetic fields is played by the rotation of magnetic moments in the vicinity of point defects (Fig. 2a,c). The further increase in the magnetisation is related to the dumping of the thermally activated spin waves (Fig. 2b,d).

Analysis of the high-field magnetisation curves in the Holstein–Primakoff paraprocess region allowed the determination of the values of the stiffness parameters of the spin waves. The value of D_{spf} is higher for the sample of $Fe_{60}Co_{10}Mo_5Cr_4Nb_6B_{15}$ alloy, which suggests a higher atomic packing density. The distances between the nearest neighbouring magnetic atoms are smaller than for the alloy containing Ni, which results in an improvement in CSRO [16].

References

[1] F.F. Marzo, A.R. Pierna, M.M. Vega, *J. Non-Cryst. Solids* **329**, 108 (2003).

[2] K. Błoch, *J. Magn. Magn. Mater.* **60**, 2019 (2015).

[3] M. Nabiałek, *J. Alloys Comp.* **642**, 98 (2015).

[4] K. Błoch, M. Nabiałek, J. Gondro, M. Szota, *Arch. Metall. Mater.* **60**, 2019 (2015).

[5] K. Błoch, M. Nabiałek, *Acta Phys. Pol. A* **127**, 442 (2015).

[6] M. Nabiałek, P. Pietrusiewicz, K. Błoch, *J. Alloys Comp.* **628**, 424 (2015).

[7] H. Kronmüller, *J. Appl. Phys.* **52**, 1859 (1981).

[8] H. Kronmüller, *IEEE Trans. Magn.* **15**, 1225 (1979).

[9] H. Kronmüller, M. Fahnle, H. Grimm, R. Grimm, B. Groger, *J. Magn. Magn. Mater.* **13**, 53 (1979).

[10] M. Vázquez, W. Fernengel, H. Kronmüller, *Phys. Status Solidi A* **115**, 547 (1989).

[11] O. Kohmoto, *J. Appl. Phys.* **53**, 7486 (1982).

[12] K. Błoch, M. Nabiałek, *Acta Phys. Pol. A* **127**, 413 (2015).

[13] T. Holstein, H. Primakoff, *Phys. Rev.* **59**, 388 (1941).

[14] K.. Błoch, M. Nabiałek, J. Gondro, *Mater. Technol.* **49**, 553 (2015).

[15] M. Szota, *Arch. Metall. Mater.* **60**, 3095 (2015).

[16] N. Lenge, H. Kronmüller, *Phys. Status Solidi A* **95**, 621 (1986).